A Generic Luczak-based Cardiovascular Model for Healthy Subjects under Physical Stress

Mohamed A.Abbass
Military Technical College
Cairo
Egypt

Emad ElSamahy
Military Technical College
Cairo
Egypt

ABSTRACT
A generic cardiovascular (CV) model for subjects under physical stress, based on luczak first and second models, is presented in this paper. A measured heart rate (HR) and blood pressure (BP) signals for 16 healthy subjects were used from a previous research, the measured data were divided into two groups: 12 subjects (Group (1)) for parameters estimation and neural network training, while the other 4 subjects (Group (2)) for model validation. The parameters were estimated via the parameter estimation toolbox (pattern search method) within the environment of Matlab®. The best parameters for each 12 subject were used as a target for an intelligent neural network layer, which used to interpolate the input features for an unknown subject to these parameters. The output of the generic model was validated by comparing the measured HR and BP signals of Group (2) and the estimated one in the frequency and time domains. Finally, the presented generic model with its intelligent neural network layer was found to be able to simulate the HR and BP signals for the unknown subjects under test with a good accuracy.

General Terms
Neural Networks and Signal Processing.

Keywords
Luczak model, cardiovascular system, parameter estimation, pattern search method, neural network, physical stress.

1. INTRODUCTION
Modeling and simulation are now a stand-alone methodology of similar value to laboratory investigations and clinical trials [1]. In this paper our work on modeling and simulation of the CV system is continued. We started with modelling the CV for healthy subjects at rest based on luczak's first model [2] , but it was not able to simulate the subjects under physical stress so some modifications were done to produce a second version [3] of that model to reach our target. Although, the second version showed better results, it still has an important disadvantage which is the estimated model parameters are specified for each subject. That means each subject has a unique model. Hence, in this paper we discuss the ability to construct a generic model that will be able to represent the behavior of a wide range of subjects' dynamics under physical stress. In order to build this model an intelligent layer should be included whose role will be mapping some selected characterizing features for the subject under test and predicting the corresponding model parameters representing this subject. The proposed generic model will be suitable for subjects with age of (35±7 years) and weight of (75.5±6 Kg).

The estimated parameters for each subject of Group (1) were used from our previous work [3] as an output for the intelligent neural network layer while its input will be the measured features (resting HR, resting BP, age and weight) from the subjects. The output of the proposed generic model was validated by comparing the measured real time HR and BP signals for a group of 4 subjects [Group (2)] against the estimated HR and BP signals in time and frequency domains. The actual real time HR and BP signals for the 4 subjects of Group (2) were acquired from a previous research [4, 5]. Figure 1 shows the block diagram of the proposed generic CV model.

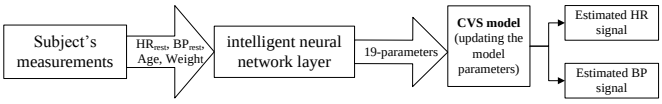

Fig 1: The block diagram of the proposed generic CV model

2. STRUCTURE OF THE PROPOSED INTELLIGENT LAYER
The function of this layer is to map the features which will be extracted from the actual measurements of the new subject, to the parameters which were estimated during the optimization procedure of the proposed model, (see Figure 2). Since it is required to have a high accuracy in the training phase, because the parameters should be exactly estimated, neural networks were selected to construct such a layer because they can afford such accuracy [6], as will be discussed later in this paper.

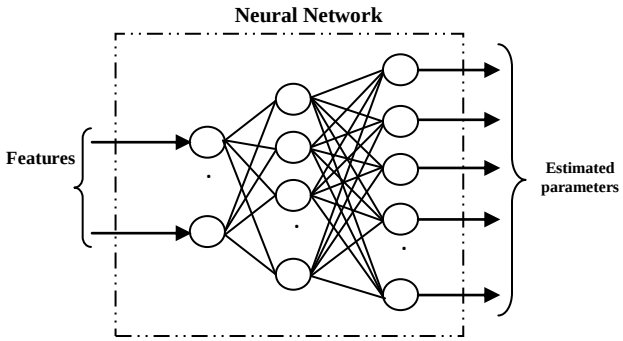

Fig 2: The Proposed intelligent neural network structure.

A detailed study was carried out to select the most appropriate type and structure of the neural network in constructing the proposed intelligent layer [6]. The most recommended neural networks types that are believed to construct such layer are as follows:

a. Feedforward neural network.
b. Generalised regression neural network (GRNN).
c. Radial basis neural network.

The previously mentioned neural networks types were evaluated by E. ElSamahy [5]. The evaluation results showed that the GRNN outperformed the other two neural networks types.

2.1 Generalized regression neural network

The GRNN was introduced by Nadaraya [7] and Watson [8] and rediscovered by Specht [9] to perform general (linear or nonlinear) regressions. The GRNN was applied to solve a variety of problems like prediction, control, plant process modeling, general mapping problems and classification [10]. Therefore, the GRNN was used to construct the proposed intelligent layer.

Moreover, the GRNN can be considered a kind of radial basis network that is often used for function approximation. A typical radial basis function is the Gaussian which is shown in Figure 3 and represented by Equation 1.

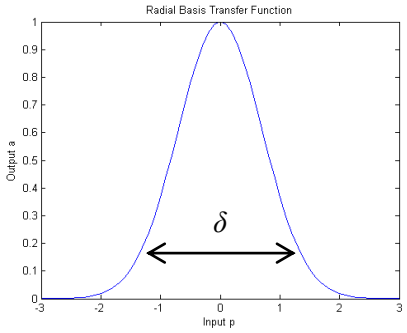

Fig 3: Radial Basis Transfer function [11].

$$h(x) = e^{-(\frac{(x-c)^2}{\delta^2})} \quad (1)$$

Where:

c: is the center.
δ: is the spread (width).

It worth noting that the GRNN has four layers which are input layer, radial basis layer, special linear layer (summation layer) and output layer.

The structure of the GRNN is based on calculating the distance between the input features vector and all the features of the training group which are stored during the training phase. The resultant vector of distances is then multiplied by the bias of radial basis layer which is 0.8326/spread (δ), such that for a smaller spread the large distances became much larger to decrease their weights in the output. Furthermore, the resultant vector is passed through the radial basis function with width equal to (δ). Hence, for smaller values of the spread (δ), a very steep function will be obtained and that results in much larger output for the input vector that is close to one of the feature vectors. Finally, the network will tend to respond with the target vector associated with the nearest vector to that input vector. In other words, for large values of spread (δ), a smoother function will be obtained, and the network then behaves as if it is calculating a weighted average between the target vectors which are close to the input vector. Conversely, for small values for the spread (δ) parameter, the output will be exactly equal to one of the stored vectors in the network structure, which are the target vectors. Therefore, a small value of the spread (δ) parameter should be used to satisfy a good accuracy over the training group (Group (1)).

It is worth noting that the output set of parameters for any new set of features will be one of the stored sets within the neural network structure. Therefore, the intelligent layer function is to select a combination from the 19 parameters from the 12 subjects of Group (1) that are stored in the intelligent layer for the new subjects. Each vector is the best matched one to the new subject according to his extracted features, which eventually can provide a qualitative behavior for that subject.

The proposed intelligent layer was introduced to the second version of the CV model under physical stress and was constructed with the Simulink® toolbox as shown in Figure 4.

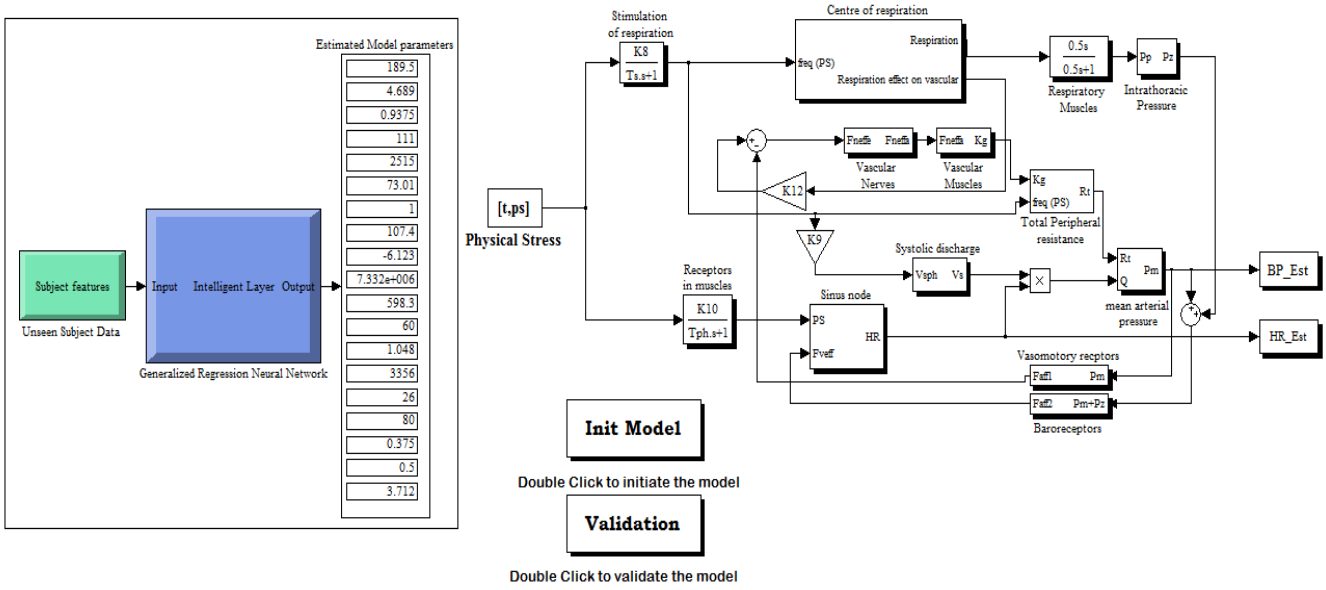

Fig 4: The proposed generic model after adding the intelligent layer.

2.2 Choosing the spread parameter "δ" value for the GRNN structure

The choice of the spread parameter (δ) value has a great influence on controlling the generalization performance of the constructed GRNN. It represents the width of the radial basis functions which exist in the first hidden layer. The larger (δ) is, the smoother the function approximation will be. In other words, to fit the data closely the spread should be set to a value smaller than the typical distance between input vectors. Conversely, a larger spread value will fit the data more smoothly and enhance the performance towards unknown subject data. So a further analysis was carried out to determine the best value for the spread parameter (δ).

Ten different values of the spread parameter (δ) were chosen to cover small values as well as large values. These values are as follows: 0.5, 0.6, 0.7, 0.8, 0.9, 1, 5, 10, 20, and 100. The effect of each spread parameter was investigated by calculating the mean squared error (MSE) of the actual and estimated HR and BP signals for the 4 subjects of Group (2). More details about the actual measurement and features of each subject in Group (2) can be found in the work done by E.ElSamahy et.al [4, 5]. the MSE is calculated as shown in Equation 2 [5].

$$MSE = \frac{1}{N}\sum_{k=1}^{N}(y_k - y_k^p)^2 \quad (2)$$

Where:

y_k: is the actual output at sample instant *k*.
y^p_k: is the predicted output at the sample instant *k*.
N: is the number of samples.

The MSE for the actual and estimated HR and BP signals of the 4 subjects in Group (2) are shown in Table 1.

Table 1.The MSE for HR and BP signals corresponding to different spread parameter values (δ)

		Subject 1		Subject 2		Subject 3		Subject 4	
		HR	**BP**	**HR**	**BP**	**HR**	**BP**	**HR**	**BP**
Spread (δ)	**0.5**	172.09	455.19	395.61	454.76	214.26	430.53	139.19	1.47e+3
	0.6	172.09	455.19	395.61	454.76	214.26	430.53	170.23	914.3491
	0.7	172.09	455.19	395.61	454.76	214.26	430.53	111.22	1.23e+3
	0.8	172.09	455.19	395.61	454.76	214.26	430.53	186.68	407.10
	0.9	172.09	455.19	395.61	454.76	182.60	356.92	136.27	578.52
	1	160.90	434.72	395.61	454.76	137.84	252.91	104.59	1.64e+3
	5	187.17	1.96e+4	397.76	992.60	170.44	1.08e+3	105.49	1.45e+4
	10	2.3e+3	3.98e+5	645.08	5.89e+5	3.27e+3	2.73e+5	2.33e+3	1.75e+5
	20	1.5e+3	1.16e+6	669.73	2.33e+6	3.16e+3	2.07e+6	1.91e+3	9.19e+5
	100	1.8e+3	2.98e+6	667.15	2.84e+6	2.01e+3	2.79e+6	1.84e+3	2.81e+6

The results shown in Table 1 exhibits that the spread values have a great effect on the MSE for both HR and BP signals especially in the case of large values of (δ) (≥ 5) for most of the subjects, which proves the importance of its proper selection. Greater values show that the performance of the closed loop model was greatly affected, which resulted from the inaccuracy of the predicted parameters. Moreover, Figure 5 shows the relation between the MSE values of the HR signal to the different spread parameter values. Also, Figure 6 shows the relation between the MSE values of the BP signal to different spread parameter values.

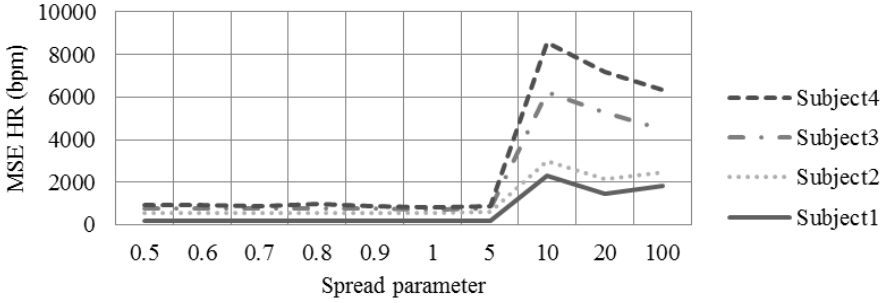

Fig 5: The MSE of HR signal for subjects in Group (2).

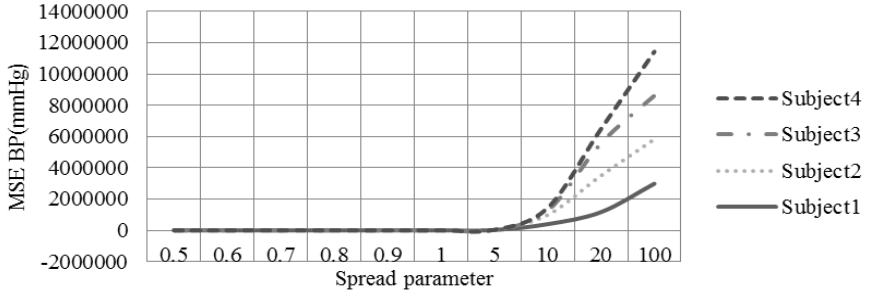

Fig 6: The MSE of the BP signal for subjects in Group (2).

As shown in Figure 5 and Figure 6, the MSE values for both BP and HR signals are nearly the same for the values less than or equal five, while it diverges to higher values for the spread parameter greater than five. However, by inspecting the results of Table 1, it can be seen that there is a considerable differences in MSE of HR and BP signals between (1) and (5). Therefore, setting the spread (δ) value to 5 will deteriorate the performance of the proposed generic model. Moreover, comparing the results of the MSE of HR and BP signals shown in Table 1 for the spread values less or equal to one, it can be seen that setting the spread value to 1 enhance the generic model performance over all the other spread values less than one except for the MSE of BP for subject 4. Hence, the spread (δ) value was chosen to be one.

3. RESULTS AND DISCUSSION

The physical extracted features of the 4 subjects in Group (2) were used as an input for the intelligent layer to predict the 19 parameters of the model for each subject. Table 2 shows the predicted parameters for each subject of Group (2).

Table 2.The predicted parameters of Group (2)

		Subject			
		1	**2**	**3**	**4**
Parameters	A_o	788.9	1979.9	189.51	709.59
	D_1	3.6861	4.4391	4.6891	3.61
	D_2	2.0556	1.3125	0.9375	2.042
	HR_o	110	110	110.99	110.01
	K_{10}	1536.3	6.5	2514.99	1416.73
	K_{11}	41.015	41.015	73.015	45.31
	K_{12}	1	1	1	1
	K_6	96.004	0.19501	107.36	85.065
	K_7	-6.2484	-6.2484	-6.1234	-6.2484
	K_8	1.091e+12	32.508	7331999.99	9.65e+11
	K_9	8192.99	682.04	598.35	7373.45
	P_o	50	50	59.99	50.02
	Rt_o	0.0479	0.2979	1.0479	0.091
	T_{ph}	36	28.275	3355.99	35.23
	T_s	9.8125	26	26	11.7
	VS_o	52.75	72.75	79.99	55.083
	K_2	0.62499	2	0.37499	0.554
	w_1	0.5	0.5	0.499	0.5
	w_2	1.7125	1.7125	3.7125	1.7125

The results of the generic model simulation for the 4 subjects in Group (2) were validated in both the time and frequency domains for both HR and BP signals. Moreover, a further analysis is carried out by calculating the correlation coefficient for the signals in time domain and the magnitude squared coherence estimate[12] for the signals in frequency domain.

Subject (2) results will be discussed in details in this section. Figure 7 shows the actual against the estimated HR signals in time domain, while Figure 8 shows the actual against the estimated BP signals in time domain. Moreover, Figure 9 shows the actual against the estimated HR signals in frequency domain, while Figure 10 shows the actual against the estimated BP signals in frequency domain.

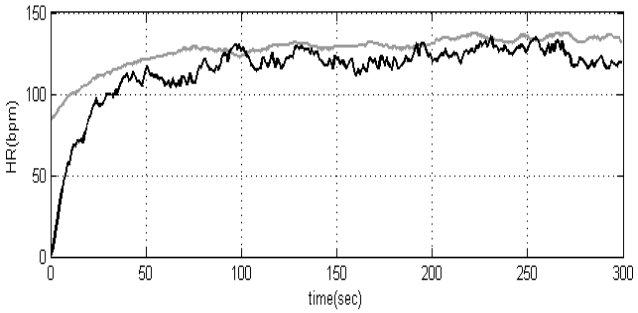

Fig 7: The measured (light) vs the estimated (dark) HR signals in time domain.

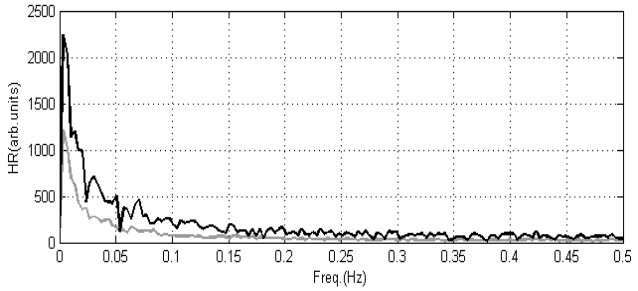

Fig 8: The measured (light) vs the estimated (dark) HR signals in frequency domain.

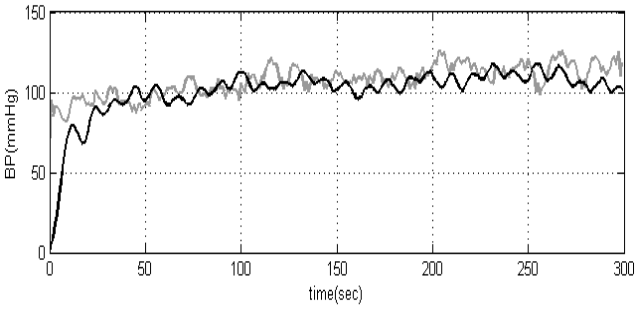

Fig 9: The measured (light) vs the estimated (dark) BP signals in time domain.

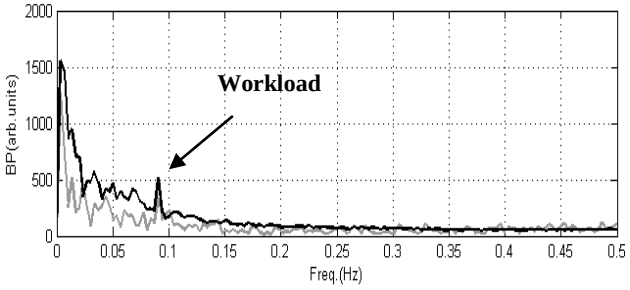

Fig 10: The measured (light) vs the estimated (dark) BP signals in frequency domain.

The frequency spectrum of Figure 10 shows how the estimated BP signal captured the most important dynamics, which existed in the actual (measured) ones. These dynamics are the workload frequency (0.091 Hz), which is an indication for the BP entrainment at that frequency.

The magnitude squared coherence estimate of the actual and estimated HR signals is shown in Figure 11(a), while the magnitude squared coherence estimate of the actual and estimated BP signals is shown in Figure 11(b).

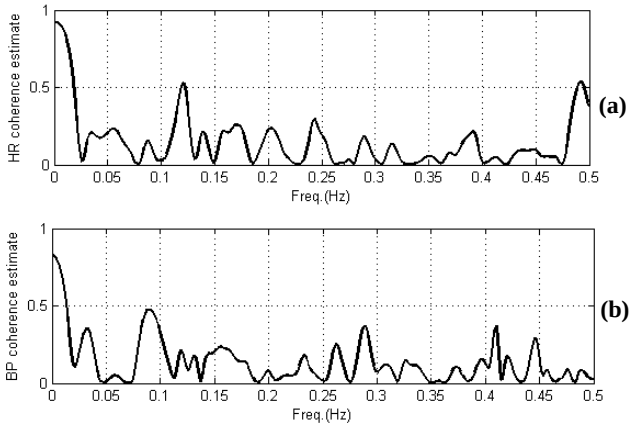

Fig 11: The magnitude squared coherence estimate for subject (2) between (a) measured and estimated HR signals, and (b) actual and estimated BP signals

Figure 11(a) and Figure 11(b) show good coherence estimate for both HR and BP signals in the LF band (almost 0.5), while for the HF frequency band the results were slightly low (almost 0.35). However, inspite of the small coherence estimate in the HF band, which is due to the high dynamics of respiratory module, the results still could be accepted of the generic model as a quantitative representation in the case of new subjects.

Therefore, the generic model can be considered as being able to capture the dynamics of the baroreflex activity as well as the respiratory activity under physical stress for new subjects with accepted accuracy.

Consequently, the proposed generic model also succeeded in estimating some other electrophysiological signals. These signals are very difficult to be acquired non-invasively and they require an invasive procedure to be extracted from the subject. Figure 12(a), (b) and (c) show some of these signals such as the sympathetic efferents, the parasympathetic efferents and the vasomotor impulses respectively.

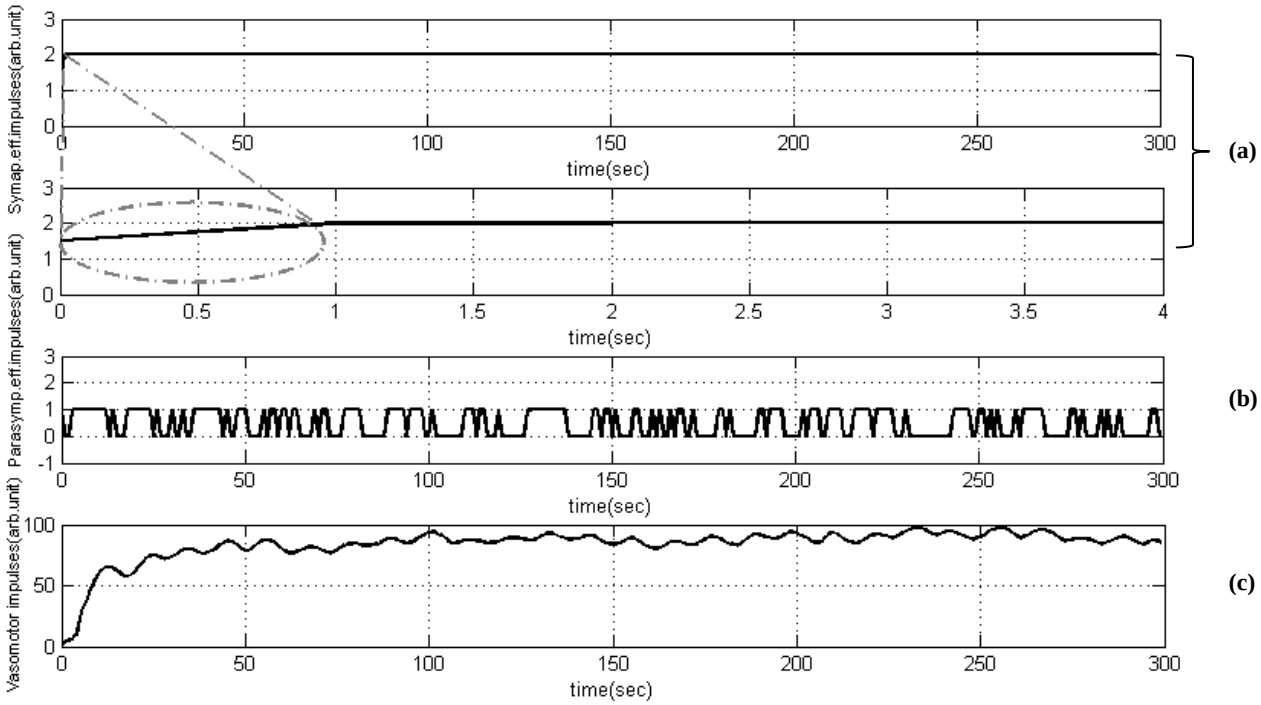

Fig 12: Some estimated electrophysiological signals from the proposed generic model under physical stress, (a) sympathetic efferent impulses, (b) parasympathetic efferent impulses, and (c) vasomotor impulses.

Figure 12 shows that the amplitude of the sympathetic signal is increased to produce increase in the HR signal and consequently the BP signal. On the other hand, there exist low dynamics in the parasympathetic signal due to the effect of the physical stress. Therefore, these results were found to agree with the physiology of the CV system under physical stress [13, 14]. Figure 13(a) and Figure 13(b) show the effect of removing the applied physical stress on the sympathetic and the parasympathetic impulses respectively.

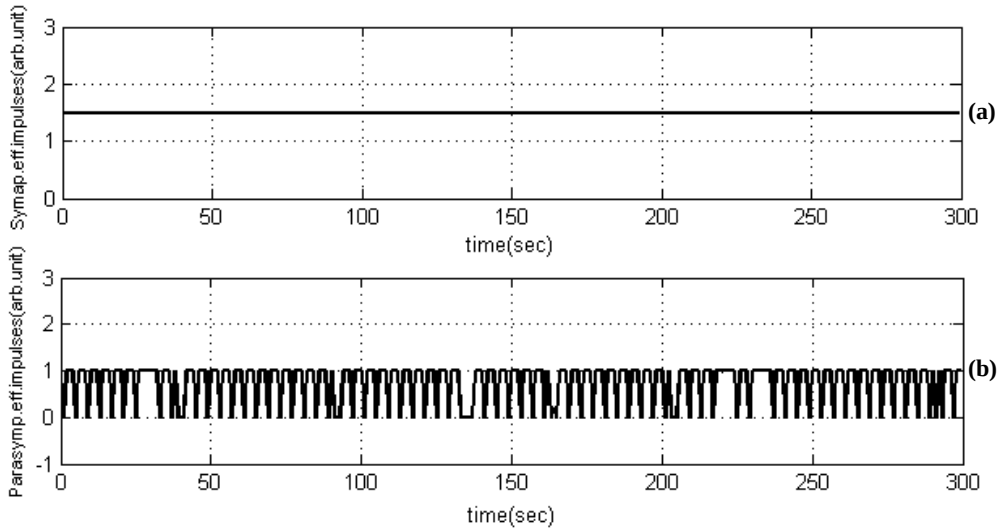

Fig 13: Some estimated electrophysiological signals from the proposed generic model with no physical stress, (a) sympathetic efferent impulses and (b) parasympathetic efferent impulses.

Figure 13(a) shows a decrease in the amplitude of the sympathetic signal, while Figure 13(b) shows an increase in the dynamics of the parasympathetic signal due to the removal of the applied physical stress, which leads to decrease in the HR and BP signals. These results were also found to agree with the physiology of the CV system.

The correlation coefficient[15] was calculated for the actual against the estimated HR and BP signals for the subjects in Group (2) as shown in Figure 14.

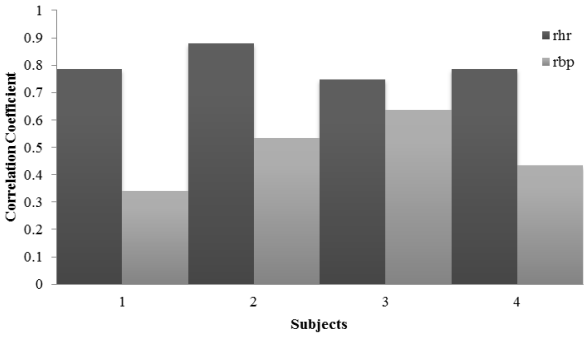

Fig 14: HR (rhr) and BP (rbp) correlation coefficients for the 4 subjects.

Figure 13 shows that the estimated HR signals from the proposed generic model are highly correlated (greater than 0.74) for all subjects. However, the estimated BP signals from the model and the actual BP signals show good correlation (greater than 0.5) for half of the subjects in Group (2). These results, as previously illustrated, are believed to be due to the existence of high dynamics which are found in the BP signals of the subjects. Moreover, these dynamics was very difficult to be modeled correctly by one model for all the 4 new subjects due to the differences existed between them.

4. CONCLUSION

Finally, a generic model for the CV system, which can be used for estimating the physiological state of unknown subjects under physical stress, was presented in this paper. The presented generic model with its intelligent neural network layer was found to be able to simulate the HR and BP signals for new subjects under physical stress with a good accuracy. Moreover, a time and frequency analyses were carried out on the model output signals, which revealed the ability of the model to simulate the baroreflex and respiratory activity with accepted accuracy. As a result of these analyses, the simulated HR signal was found to be modeled more accurate than the simulated BP signal, which is resulted from the high dynamics existed in the BP signal compared to the HR signal. In the future, a detailed study will be carried out on exploiting the constructed model in some useful medical and sport applications.

5. REFERENCES

[1] W. v. Meurs, Modeling and Simulation in Biomedical Engineering: Applications in Cardiorespiratory Physiology: McGraw Hill, 2011.

[2] Mohamed A. Abbass, et al., "An Optimized Cardiovascular Model: A pattern Search approach," in 2012 International Conference on Biomedical Engineering and Biotechnology, Macau,China, 2012, pp. 45-48.

[3] Mohamed A. Abbass, et al., "Modeling and Simulation of the Cardiovascular System for Healthy Subjects under Physical Stress " in 2012 6th Cairo International Biomedical Engineering Conference Cairo, Egypt, 2012.

[4] E. El-Samahy, Mahdi Mahfouf and Derek A.Linkens "A closed-loop hybrid physiological model relating to subjects under physical stress," Artificial Intelligence in Medicine, vol. 38, pp. 257-274, 2006.

[5] E. Elsamahy, "A Generic Grey-box Model for the Cardiovascular System of Subjects Experiencing Physical Stress," Doctor of Philosophy, Automatic Control and Systems Engineering, Sheffield, 2003.

[6] L. H. Tsoukalas and R. E. Uhrig, Fuzzy and neural approaches in engineering: Wiley, 1997.

[7] E. A. Nadaraya, "On estimating regression," Theory of Probab. Applicat., vol. 9, pp. 141–142, 1964.

[8] G. S. Watson, "Smooth regression analysis," Sankhya Series A, vol. 26, pp. 359–372, 1964.

[9] D. F. Specht, "A General Regression Neural Network," IEEE TRANSACTIONS ON NEURAL NETWORKS, vol. 2, Novamber 1991.

[10] E. Al-Daoud, "A Comparison Between Three Neural Network Models for Classification Problems," Jounal of Artificial Intelligence, vol. 2, pp. 56-64, 2009.

[11] Neural Network Toolbox. Available: http://www.mathworks.com/help/toolbox/nnet/ug/bss38j0-1.html

[12] Signal Processing Toolbox. Available: http://www.mathworks.com/help/toolbox/signal/ref/mscohere.html

[13] A. C. Guyton , John E. Hall, TEXTBOOK OF MEDICAL PHYSIOLOGY, eleventh ed.: Elsevier Inc., 2006.

[14] S. S. Mader, Mader: Understanding Human Anatomy & Physiology, Fifth ed.: The McGraw−Hill Companies, 2004.

[15] Statistics Toolbox. Available: http://www.mathworks.com/help/toolbox/stats/corr.html